Inorganica Chimica Acta 408 (2013) 152–161

Contents lists available at ScienceDirect

Inorganica Chimica Acta

journal homepage: www.elsevier.com/locate/ica

Dinuclear zinc bis(thiosemicarbazone) complexes: Synthesis, *in vitro* anticancer activity, cellular uptake and DNA interaction study

Duraippandi Palanimuthu, Ashoka G. Samuelson *

Department of Inorganic and Physical Chemistry, Indian Institute of Science, Bangalore 560012, India

ARTICLE INFO

Article history:
Received 18 July 2013
Received in revised form 2 September 2013
Accepted 4 September 2013
Available online 12 September 2013

Keywords:
Bis(thiosemicarbazone)
Zinc
Dinuclear complex
Anticancer activity
DNA binding
Cellular uptake

ABSTRACT

Four dinucleating bis(thiosemicarbazone) ligands and their zinc complexes have been synthesized and characterized by multinuclear NMR (^{1}H and ^{13}C), IR, UV–Vis, ESI-MS and fluorescence spectroscopic techniques. Their purity was assessed by elemental analysis. Cytotoxicity was tested against five human cancer cell lines using the sulphorhodamine B (SRB) assay, where one of the complexes, 1,3-bis{biacetyl-2′-(4″-N-pyrrolidinylthiosemicarbazone)-3′-(4″-N-pyrrolidinylthiosemicarbazone)zinc(II)}propane (**6**), was found to be quite cytotoxic against MCF-7 (breast cancer) and HepG2 (hepatoma cancer) cell lines, with a potency similar to that of the well known anticancer drug adriamycin. It is evident from the cellular uptake studies that the uptake is same for the active complex **6** and the inactive complex **8** (1,6-bis{biacetyl-2′-(4″-N-pyrrolidinylthiosemicarbazone)-3′-(4″-N-pyrrolidinylthiosemicarbazone)zinc(II)}hexane) in MCF-7 and HepG2 cell lines. *In vitro* DNA binding and cleavage studies revealed that all complexes bind with DNA through electrostatic interaction, and cause no significant cleavage of DNA.

© 2013 Elsevier B.V. All rights reserved.

1. Introduction

The use of transition metal complexes in cancer therapy has gained importance from the time it was discovered that cis-diamminedichloroplatinum(II) (cisplatin) was anticancer active [1,2]. A variety of mononuclear metal complexes with different ligands have been shown to be effective for cancer therapy both *in vitro* and *in vivo* [3–7]. Some of the metal complexes including cisplatin, carboplatin and oxaliplatin have been approved by FDA and are currently being used worldwide to treat various cancers [8,9]. Nine transition metal complexes with platinum, gold and ruthenium metal centers are under various stages of clinical trials and in the last two years two platinum complexes and a palladium complex have entered clinical trials [10–12].

Mounting evidence in the literature shows that dinuclear and multinuclear complexes are more efficacious than the corresponding mononuclear complexes in terms of their cellular uptake, cytotoxicity, DNA binding and DNA cleavage [13–17]. A typical example is BBR3464, a trinuclear platinum complex (Fig. 1), which rendered 10–100 times higher cytotoxicity than the monomeric analogue cisplatin (Fig. 1) due to its unique DNA binding property [15]. Recently, Wang and coworkers demonstrated that when two nontoxic mononuclear ruthenium complexes (B in Fig. 1) bearing bipyridyl ligands are linked together by a thiophene ligand (A in Fig. 1), the cytotoxicity is dramatically enhanced by many folds owing to their strong DNA binding [18]. More recently, Spingler and coworkers have shown that the dinuclear nickel and copper complexes containing 1,3-bis(1,5,9-triazacyclododecyl)propane ligand (C in Fig. 1) are able to change the conformation of right-handed B-DNA into left-handed Z-DNA, whereas the corresponding mononuclear complexes (D in Fig. 1) fail to bring such a conformational change [19]. Therefore developing dinuclear or multinuclear complexes and their comparison with mononuclear analogs is quite interesting due to their enhanced anticancer activity and interactions with biomolecules.

Transition metal bis(thiosemicarbazones), a class of metal complexes, have been of great interest due to the wide range of biological activities they exhibit, this includes anti-alzheimer's, anti-malarial, anti-bacterial, anti-viral and anti-cancer activity [20–24]. In recent years, zinc and copper bis(thiosemicarbazone) complexes have attracted attention due to their intracellular fluorescence and anticancer activity, respectively [25,26]. A few reports have shown that zinc complexes of mono- and bis-thiosemicarbazone ligands exhibit both anticancer activity and fluorescence

Abbreviations: $GTSCH_2$, glyoxal-bis(4-methyl-4-phenyl-3-thiosemicarbazone); $ATSMH_2$, biacetyl-bis(4-methyl-3-thiosemicarbazone); $[Zn(GTSC)]_3$, zinc glyoxal-bis(4-methyl-4-phenyl-3-thiosemicarbazone); HRMS, high-resolution mass spectra; EB, ethidium bromide; CT, calf-thymus; NC, nicked-circular; SC, supercoiled; EDTA, ethylenediaminetetraacetic acid; MTT, 3-(4,5-dimethylthiazol-2-yl)-2,5-diphenyltetrazolium bromide; SRB, sulphorhodamine B; bpy, 2,2′-bipyridine; phen, 1,10-phenanthroline; PBS, phosphate buffered saline; Tris–HCl, tris(hydroxymethyl)aminomethane–hydrochloride; HEPES, 4-(2-hydroxyethyl)-1-piperazineethanesulfonic acid.

* Corresponding author. Tel.: +91 80 2293 2663; fax: +91 80 2360 1552.
E-mail address: ashoka@ipc.iisc.ernet.in (A.G. Samuelson).

0020-1693/$ - see front matter © 2013 Elsevier B.V. All rights reserved.
http://dx.doi.org/10.1016/j.ica.2013.09.014

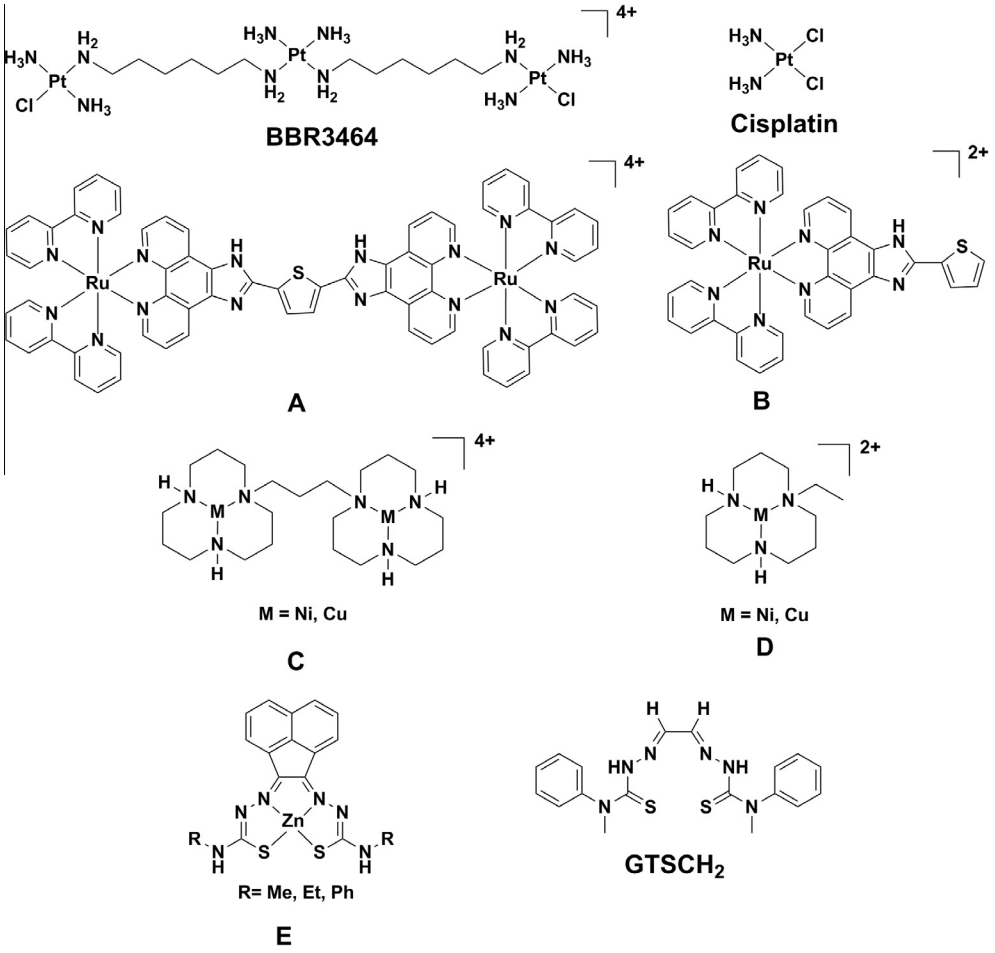

Fig. 1. Structures of metal complexes and the ligand, $GTSCH_2$, referred to in the introduction.

imaging property [27,28]. For example, Pascu and coworkers documented that acenaphthenequinone based zinc bis(thiosemicarbazone) complexes (E in Fig. 1) exhibited comparable cytotoxicity to cisplatin in the MCF-7 cell line and emitted fluorescence as well [28]. Recently, we reported synthesis and biological characterization of a range of bis(thiosemicarbazone) ligands and their mononuclear copper and zinc complexes. We showed that one of the ligands, $GTSCH_2$ [glyoxal-bis(4-methyl-4-phenyl-3-thiosemicarbazone)] (Fig. 1), is suitable for imaging cellular zinc and the corresponding zinc complex is suitable for imaging several cancer cell lines of different tissue origin [29,30]. And interestingly, many of the copper complexes are found to be anticancer active [31]. Several reports including ours have proven that small modifications in the structure of metal bis(thiosemicarbazone) complexes lead to significant changes in their anticancer activity and their fluorescence property [25,30–32].

Synthesis and characterization of a few dinuclear zinc bis(thiosemicarbazone) complexes, where the bis(thiosemicarbazone) ligands are coupled through an organic linker or where the two zinc atoms are linked through a bridging sulfur, have been reported [33–37]. However no anticancer activity has been evaluated for these dinuclear compounds. Based on these observations, we felt that dinuclear zinc bis(thiosemicarbazone) complexes would have interesting biological properties. We have synthesized a series of dinuclear zinc bis(thiosemicarbazone) complexes by varying substituents on the thiosemicarbazide part of the ligand and varying the length of the bridging diaminoalkane. Their characterization and structural influence on anticancer activity and imaging potential is also reported. Cytotoxicity has been evaluated in five cancer cell lines of different tissue origin. The cellular uptake was investigated by estimating the amount of accumulation of zinc in two cell lines using ICP-OES. The ability of zinc complexes to fluoresce within HepG2 cells has been examined by flow cytometry. Effects of these complexes on DNA binding and DNA cleavage have been investigated by the ethidium bromide displacement assay, viscosity analysis, circular dichroism experiments and agarose gel electrophoresis. Although most properties of dinuclear complexes are similar to mononuclear complexes, the cytotoxicity of the propylenediamine bridged dinuclear zinc complex is as high as adriamycin, a potent anticancer drug.

2. Experimental

2.1. Materials and methods

All reagents and solvents were purchased from either Aldrich (USA) or Merck (India) or Spectrochem (India) and used without further purification. 1,3-diaminopropane and CS_2 were purified by standard methods prior to use. ^1H and $^{13}C\{^1H\}$ NMR spectra were recorded on a Bruker AMX 400 spectrometer operating at 400 MHz for ^1H and 100.6 MHz for ^{13}C NMR with tetramethylsilane as an internal standard. Infrared spectra were recorded on a Bruker ALPHA10 FT-IR spectrometer operating on an ATR mode. All UV–Vis and fluorescence spectra were recorded on PerkinElmer (Lambda 750) and Horiba Jobin Yvon (FluoroMax-4) spectrofluo-

rometer, respectively. Mass spectra were recorded on an Agilent 6538 UHD Accurate-Mass QTOF-LC/MS instrument. Elemental analyses were carried out using a Thermo Finnigan Flash EA 2000 CHNS analyzer. Molar conductivity measurements were carried out on a Control Dynamics conductivity meter. Zinc standard (ICP grade) was purchased from Fluka for the Inductively Coupled Plasma-Optical Emission Spectroscopy (ICP-OES) and the amount of zinc in cells was estimated by PerkinElmer Optima 2000 DV. Supercoiled (SC) pBR322 DNA (cesium chloride purified) was purchased from Bangalore Genie (India). Calf-thymus DNA was procured from Sigma (India). All reagents used for the cell culture, MTT assay and DNA binding and cleavage experiments were obtained from Sigma (USA).

2.2. Syntheses

2.2.1. Mono-keto-(propane-1,3-dithiosemicarbazone)

Propane-1,3-dithiosemicarbazide (0.40 g, 1.8 mmol) and 2,3-butanedione (0.41 g, 4.7 mmol) were added to water (20 mL) containing conc. HCl (0.4 mL) and stirred for 30 min at room temperature. The precipitate formed was collected by filtration, washed with water and dried in air to obtain 0.42 g of the white solid. Yield: 67%. ^{1}H NMR (400 MHz, d^6-DMSO): δ 1.90 (2H, t, CH_2), δ 1.97 (6H, s, CH_3–C=N), δ 2.43 (6H, s, CH_3–C=O), δ 3.66–3.70 (4H, q, CH_2–NH), δ 8.82 (2H, t, NH–CH$_2$, linker), δ 10.68 (2H, s, NH). ^{13}C NMR (100.6 MHz, d^6-DMSO): δ 11.0 (*C*H$_3$–C=N), δ 25.8 (*C*H$_3$–C=O), δ 29.4 (*C*H$_2$), δ 42.1 (*C*H$_2$–NH), δ 146.8 (*C*=N), δ 179.3 (*C*=S), δ 198.3 (*C*=O). IR Data/cm^{-1}: 3345 (m), 3245 (m, NH), 3236 (m, NH), 2936 (m), 2352 (m), 1675 (s, C=O), 1594 (m), 1539 (s), 1487 (s), 1237 (vs thioamide), 1172 (s), 1141(m), 964 (m).

2.2.2. Mono-keto-(hexane-1,6-dithiosemicarbazone)

Hexane-1,6-dithiosemicarbazide (2.5 g, 9.46 mmol) was added to water (50 mL) containing conc. HCl (2.2 mL) and stirred until it dissolved completely. The addition of 2,3-butanedione (2.4 g, 27.37 mmol) brought about the immediate precipitation of the desired product which was collected by filtration, washed with water and dried in air to get 3.3 g of the white solid. Yield: 86%. ^{1}H NMR (400 MHz, d^6-DMSO): δ 1.34 (4H, t, CH_2), δ 1.60 (4H, quintet, CH_2), δ 1.95 (6H, s, CH_3–C=N), δ 2.41 (6H, s, CH_3–C=O), δ 3.59 (4H, q, CH_2–NH), δ 8.65 (2H, t, NH–CH$_2$), δ 10.59 (2H, t, NH). ^{13}C NMR (100.6 MHz, d^6-DMSO): δ 10.9 (*C*H$_3$–C=N), 25.7 (*C*H$_3$–C=O), 27.1 (CH$_2$), δ 29.3 (*C*H$_2$), δ 44.8 (*C*H$_2$–NH), δ 146.4 (*C*=N), δ 179.1 (*C*=S), δ 198.4 (*C*=O). IR Data/cm^{-1}: 3249 (m, NH), 2981 (m), 2849 (m), 1620 (m, C=O), 1496 (s), 1262 (m, thioamide), 1178 (s), 1063(m), 945 (m).

2.2.3. 1,3-Bis{biacetyl-2′-(4″-N-thiosemicarbazone)-3′-(4″-N-thiosemicarbazone)}propane (**1**)

A methanolic solution (15 mL) of mono-keto-(propane-1,3-dithiosemicarbazone) (200 mg, 0.56 mmol) was refluxed for 1 h and then thiosemicarbazide (110 mg, 1.2 mmol) and glacial acetic acid (0.5 mL) were added. The resulting suspension was refluxed for 4 h. After cooling to room temperature, the product was filtered, washed with methanol and dried *in vacuo*. The product was isolated as a cream coloured solid (265 mg). Yield: 94%. ^{1}H NMR (400 MHz, d^6-DMSO): δ 1.82 (2H, quintet, CH_2), δ 2.17 (6H, s, CH_3–C=N), δ 2.22 (6H, s, CH_3–C=N), δ 3.65 (4H, q, CH_2–NH), δ 7.87 (2H, s, NH_2), δ 8.43 (2H, s, NH_2), δ 8.64 (2H, t, NH–CH$_2$, linker), δ 10.25 (2H, s, NH), δ 10.29 (2H, s, NH). ^{13}C NMR (100.6 MHz, d^6-DMSO): δ 12.6 (*C*H$_3$–C=N), 12.7 (*C*H$_3$–C=N), δ 29.9 (*C*H$_2$), δ 41.7 (*C*H$_2$-NH), δ 149.1 (*C*=N), δ 149.3 (*C*=N), δ 178.7 (*C*=S), δ 179.8 (*C*=S). HRMS (+ESI) found mass: 503.1512. Calc. mass for $C_{15}H_{29}N_{12}S_4$ (100%, [M+H$^+$]$^+$): 503.1515. *Anal.* Calc. for $C_{15}H_{28}N_{12}S_4{\cdot}3H_2O$ (%): C, 32.24; H, 6.13; N, 30.08; S, 22.95. Found: C, 32.91; H, 5.76; N, 28.91; S, 22.32%. IR Data/cm^{-1}: 3237 (m, NH), 3156 (m, NH), 1610 (m), 1541 (m, C=N), 1425 (s), 1406 (vs), 1244 (s, thioamide), 1192 (s), 1085 (vs), 837 (m, CS), 487 (m). UV–Vis (DMSO): $\lambda_{max}(\varepsilon)$ = 338 nm (60800 M^{-1} cm^{-1}).

2.2.4. 1,3-Bis{biacetyl-2′-(4″-N-pyrrolidinethiosemicarbazone)-3′-(4″-N-thiosemicarbazone)} propane (**2**)

Ligand **2** was prepared following the procedure described for preparing ligand **1** except that 4-pyrrolidinylthiosemicarbazide (460 mg, 1.28 mmol) was used instead of thiosemicarbazide, mono-keto-(propane-1,3-dithiosemicarbazone) (460 mg, 3.45 mmol) and glacial acetic acid (1 mL). The product was isolated as a yellow powder (500 mg). Yield: 64%. ^{1}H NMR (400 MHz, d^6-DMSO): δ 1.87 (10H, bs, 4 × CH_2, pyrrolidine, 1 × CH_2, linker), δ 2.14 (6H, s, CH_3–C=N), δ 2.22 (6H, s, CH_3–C=N), δ 3.65 (4H, q, CH_2–NH, linker), δ 3.71 (8H, bs, CH_2–N, pyrrolidine), δ 8.63 (2H, t, NH–CH$_2$, linker), δ 9.52 (2H, s, NH), δ 10.29 (2H, s, NH). ^{13}C NMR (100.6 MHz, d^6-DMSO): δ 12.0 (*C*H$_3$–C=N), δ 12.5 (*C*H$_3$–C=N), δ 24.5–26.9 (*C*H$_2$, broad, pyrrolidine), δ 30.0 (*C*H$_2$, linker), δ 41.8 (*C*H$_2$–NH, linker), δ 52.0–54.3 (*C*H$_2$-N, broad, pyrrolidine), δ 149.4 (*C*=N), δ 149.7 (*C*=N), δ 178.3 (*C*=S), δ 178.7 (*C*=S). HRMS (+ESI) found mass: 613.2454. Calc. mass for $C_{23}H_{41}N_{12}S_4$ (100%, [M+H$^+$]$^+$): 613.2440. *Anal.* Calc. for $C_{23}H_{40}N_{12}S_4{\cdot}2H_2O$ (%): C, 42.57; H, 6.83; N, 25.90; S, 19.77. Found: C, 42.92; H, 6.34; N, 25.61; S, 20.81%. IR Data: IR Data/cm^{-1}: 2923 (w), 2863 (w), 1625 (w), 1525 (vs C=N),1433 (w, thioamide), 1343 (s), 1277 (s), 1249 (vs), 1188 (s), 1122 (s), 898 (w, CS), 791 (w), 572 (m). UV–Vis (DMSO): $\lambda_{max}(\varepsilon)$ = 337 nm (38500 M^{-1} cm^{-1}).

2.2.5. 1,6-Bis{biacetyl-2′-(4″-N-thiosemicarbazone)-6′-(4″-N-thiosemicarbazone)}hexane (**3**)

To a stirred suspension of mono-keto-(hexane-1,6-dithiosemicarbazone) (500 mg, 1.25 mmol) in ethanol (30 mL) thiosemicarbazide (240 mg, 2.64 mmol) followed by glacial acetic acid (0.9 mL) were added and refluxed for 24 h. After cooling the solution to room temperature, the precipitate that formed was collected by filtration, washed with ethanol and dried *in vacuo*. A light yellow solid was obtained (430 mg). Yield: 63%. ^{1}H NMR (400 MHz, d^6-DMSO): δ 1.31 (4H, bs, CH_2), δ 1.58 (4H, bs, CH_2), δ 2.16 (6H, s, CH_3–C=N), δ 2.20 (6H, s, CH_3–C=N), δ 3.59 (4H, q, CH_2–NH), δ 7.86 (2H, s, NH_2), δ 8.39–8.42 (4H, m, 2 × NH–CH$_2$ and NH_2), δ 10.16 (2H, s, NH, linker), δ 10.22 (2H, s, NH). ^{13}C NMR (100.6 MHz, d^6-DMSO): δ 12.4 (*C*H$_3$–C=N), 12.6 (*C*H$_3$–C=N), δ 27.0 (*C*H$_2$), δ 29.5 (*C*H$_2$), δ 44.6 (*C*H$_2$–NH), δ 148.8 (*C*=N), δ 149.3 (*C*=N), δ 178.5 (*C*=S), δ 179.7 (*C*=S). HRMS (+ESI) found mass: 547.1982. Calc. mass for $C_{18}H_{35}N_{12}S_4$ (100%, [M+H$^+$]$^+$): 547.1985. *Anal.* Calc. for $C_{18}H_{34}N_{12}S_4{\cdot}H_2O$ (%): C, 38.27; H, 6.07; N, 29.74; S, 23.69. Found: C, 38.28; H, 6.42; N, 29.76; S, 22.72%. IR Data/cm^{-1}: 3404 (m), 3183 (m, NH), 3150 (m), 2933 (m), 2858 (w), 1596 (s), 1488 (vs C=N), 1291 (s, thioamide), 1191 (m), 1083 (s), 831 (m, CS), 500 (m). UV–Vis (DMSO): $\lambda_{max}(\varepsilon)$ = 338 nm (52700 M^{-1} cm^{-1}).

2.2.6. 1,6-Bis{biacetyl-2′-(4″-N-pyrrolidinylthiosemicarbazone)-3′-(4″-N-pyrrolidinylthiosemi carbazone)}hexane] (**4**)

Ligand **4** was prepared following the procedure used for preparing **3**, except that 4-pyrrolidinylthiosemicarbazide (0.54 g, 3.72 mmol) was used instead of thiosemicarbazide, conc. HCl (0.4 mL) and mono-keto-(propane-1,3-dithiosemicarbazone) (0.4 g, 0.95 mmol). The product was isolated as a yellow powder (500 mg). Yield: 80% (Purity of the compound is 90% as determined by ^{1}H NMR, and the remaining 8% has the unreacted mono-keto-(hexane-1,6-dithiosemicarbazone). ^{1}H NMR (400 MHz, d^6-DMSO): δ 1.33 (4H, bs, CH_2, linker), δ 1.59 (4H, bs, CH_2, linker), δ 1.91 (8H, bs, CH_2, pyrrolidine), δ 2.13 (6H, s, CH_3–C=N), δ 2.18 (6H, s, CH_3–C=N), δ 3.54 (4H, q, CH_2–NH, linker), δ 3.68 (8H, t, CH_2–NH, pyrrolidine), δ 8.38 (2H, t, NH–CH$_2$, linker), δ 9.46 (2H, s, NH), δ

10.15 (2H, s, N*H*). ^{13}C NMR (100.6 MHz, d^6-DMSO): δ 12.0 (*C*H$_3$–C=N), δ 12.5 (*C*H$_3$–C=N), δ 25.5 (*C*H$_2$, pyrrolidine), δ 26.1 (*C*H$_2$, pyrrolidine), δ 27.1 (*C*H$_2$, linker), δ 29.6 (*C*H$_2$, linker), δ 44.6 (*C*H$_2$–NH, linker), δ 52.1 (*C*H$_2$–N, pyrrolidine), δ 54.1 (*C*H$_2$–N, pyrrolidine), δ 148.9, (*C*=N), δ 149.7, (*C*=N), δ 178.3 (*C*=S), δ 178.5 (*C*=S). HRMS (+ESI) found mass: 677.2710. Calc. mass for $C_{26}H_{46}N_{12}S_4Na$ (100%, $[M+Na^+]^+$): 677.2743. *Anal.* Calc. for $C_{26}H_{46}N_{12}S_4{\cdot}2H_2O$ (%): C, 45.19; H, 7.29; N, 24.32; S, 18.56. Found: C, 45.50; H, 6.91; N, 24.18; S, 18.85%. IR Data/cm^{-1}: 3316 (m), 3175 (m, NH), 2933 (m), 2933 (m), 2861 (m), 2359 (m), 1487 (vs C=N), 1209 (vs thioamide), 1132 (vs), 550 (m). UV–Vis (DMSO): $\lambda_{max}(\varepsilon)$ = 338 nm (47 500 M^{-1} cm^{-1}).

2.2.7. 1,3-Bis{biacetyl-2′-(4″-N-thiosemicarbazone)-3′-(4″-N-thiosemicarbazone)zinc(II)} propane (**5**)

2.2.7.1. General procedure for synthesizing zinc complexes. Ligand **1** (80 mg, 0.16 mmol) and zinc acetate (75 mg, 0.37 mmol) were suspended in ethanol (10 mL) and refluxed for 8 h. The yellow precipitate formed was collected by filtration, washed with ethanol and diethylether and dried *in vacuo*. The product **5** was obtained as a pale yellow solid (52 mg).Yield: 52%. ^{1}H NMR (400 MHz, d^6-DMSO): δ 1.76 (2H, bs, C*H*$_2$), δ 2.15 (6H, s, C*H*$_3$–C=N), δ 2.19 (6H, s, C*H*$_3$–C=N), δ 3.40–3.44 (4H, bs, C*H*$_2$–NH), δ 6.89 (4H, s, N*H*$_2$), δ 7.22 (2H, bs, N*H*, linker). ^{13}C NMR (100.6 MHz, d^6-DMSO): δ 14.8 (*C*H$_3$–C=N), δ 15.0 (*C*H$_3$–C=N), δ 29.7 (*C*H$_2$), δ 40.0–41.0 (*C*H$_2$–N, merged with DMSO) δ 145.0 (*C*=N), δ 146.2 (*C*=N), δ 176.2 (*C*S), δ 178.9 (*C*S). HRMS (+ESI) found mass: 632.9725. Calc. mass for $C_{15}H_{25}N_{12}S_4Zn_2$ (100%, $[M+H^+]^+$): 632.9735. *Anal.* Calc. for $C_{15}H_{24}N_{12}S_4Zn_2{\cdot}0.5H_2O$ (%): C, 28.12; H, 3.93; N, 26.24; S, 20.02. Found: C, 28.63; H, 4.37; N, 24.18; S, 19.62%. IR Data/cm^{-1}: 3278 (w, NH), 3174 (w, NH), 2358 (w), 1617 (s), 1544 (m), 1488 (s, C=N), 1428 (vs), 1209 (s thioamide), 833 (m, CS), 727 (m). UV–Vis (DMSO): $\lambda_{max}(\varepsilon)$ = 312, 435 nm (17 100, 16 700 M^{-1} cm^{-1}).

2.2.8. 1,3-Bis{biacetyl-2′-(4″-N-pyrrolidinylthiosemicarbazone)-3′-(4″-N-pyrrolidinylthiosemi carbazone)zinc(II)}propane (**6**)

Complex **6** was prepared according to the general procedure described for **5** using zinc acetate (80 mg, 0.36 mmol) and **2** (100 mg, 0.16 mmol) in ethanol (10 mL) to afford the desired product as a yellow solid (75 mg).Yield: 63%. ^{1}H NMR (400 MHz, d^6-DMSO): δ 1.76 (2H, quintet, C*H*$_2$, linker), 1.85 (8H, bs, C*H*$_2$, pyrrolidine), δ 2.18 (6H, s, C*H*$_3$–C=N), δ 2.20 (6H, s, C*H*$_3$–C=N), δ 3.47 (4H, bs, C*H*$_2$–N, linker), δ 3.58 (8H, bs, C*H*$_2$–N, pyrrolidine), δ 7.19 (2H, bs, N*H*, linker). ^{13}C NMR (100.6 MHz, d^6-DMSO): δ 14.6 (*C*H$_3$–C=N), δ 14.9 (*C*H$_3$–C=N), 25.4 (*C*H$_2$, linker), 29.8 (*C*H$_2$, pyrrolidine), δ 39.6–40.73 (*C*H$_2$–NH, merged with DMSO, linker), δ 49.5 (*C*H$_2$–N, pyrrolidine), δ 144.9 (*C*=N), δ 175.5 (*C*=S). HRMS (+ESI) found mass: 741.0678. Calc. mass for $C_{23}H_{37}N_{12}S_4Zn_2$ (100%, $[M+H^+]^+$): 741.0677. *Anal.* Calc. for $C_{23}H_{36}N_{12}S_4Zn_2{\cdot}H_2O$ (%): C; 36.46; H, 5.06; N, 22.18; S, 16.93. Found: C, 36.51; H, 4.80; N, 21.80; S, 16.79%. IR Data/cm^{-1}: 3296 (w, NH), 2938 (w, NH), 2866 (m), 1487 (w, C=N), 1434 (vs thioamide), 1286 (m), 835 (w, CS), 744 (w), 622 (w). UV–Vis (DMSO): $\lambda_{max}(\varepsilon)$ = 316,445 nm (15 300, 16 500 M^{-1} cm^{-1}).

2.2.9. 1,6-Bis{biacetyl-2′-(4″-N-thiosemicarbazone)-6′-(4″-N-thiosemicarbazone)zinc(II)} hexane (**7**)

Complex **7** was prepared according to the general procedure described for **5** using zinc acetate (140 mg, 0.63 mmol) and **3** (170 mg, 0.31 mmol) in ethanol (15 mL) to give the product as a pale yellow solid (175 mg). Yield: 84%. ^{1}H NMR (400 MHz, d^6-DMSO): δ 1.28 (4H, bs, C*H*$_2$), δ 1.51 (4H, bs, C*H*$_2$), δ 2.15 (6H, s, C*H*$_3$–C=N), δ 2.18 (6H, s, C*H*$_3$–C=N), δ 3.27 (4H, C*H*$_2$–NH), δ 6.88 (4H, bs, N*H*$_2$), δ 7.22 (2H, bs, N*H*, linker). ^{13}C NMR (100.6 MHz, d^6-DMSO): δ 14.8 (*C*H$_3$–C=N), 14.9 (*C*H$_3$–C=N), δ 27.3 (*C*H$_2$), δ 29.8 (*C*H$_2$), δ 43.0 (*C*H$_2$–NH, linker), δ 145.2 (*C*=N), δ 178.9 (*C*S). HRMS (+ESI) found mass: 675.0228. Calc. mass for $C_{18}H_{31}N_{12}S_4Zn_2$ (100%, $[M+H^+]^+$): 675.0206. *Anal.* Calc. for $C_{18}H_{30}N_{12}S_4Zn_2{\cdot}3H_2O$ (%): C, 29.71; H, 4.98; N, 23.10; S, 17.63. Found: C, 29.61; H, 4.41; N, 22.50; S, 18.24%. IR Data/cm^{-1}: 3223 (w, NH), 3173 (w, NH), 2928 (m), 2858 (w), 1424 (vs C=N), 1364 (m), 1295 (m, thioamide), 1209 (s), 1179 (s), 1136 (m), 831 (m, CS), 710 (m). UV–Vis (DMSO): $\lambda_{max}(\varepsilon)$ = 310, 435 nm (14 500, 13 300 M^{-1} cm^{-1}).

2.2.10. 1,6-Bis{biacetyl-2′-(4″-N-pyrrolidinylthiosemicarbazone)-3′-(4″-N-pyrrolidinylthiosemi carbazone)zinc(II)} hexane (**8**)

Complex **8** was prepared according to the general procedure described for preparing **5** using zinc acetate (67 mg, 0.31 mmol) and **4** (100 mg, 0.15 mmol) in ethanol (10 mL). The product was obtained as a yellow solid (88 mg). Yield: 75%. ^{1}H NMR (400 MHz, d^6-DMSO): δ 1.28 (4H, bs, C*H*$_2$, linker), δ 1.52 (4H, bs, C*H*$_2$, linker), δ 1.85 (8H, bs, C*H*$_2$, pyrrolidine), 2.16 (6H, s, C*H*$_3$–C=N), 2.17 (6H, s, C*H*$_3$–C=N), δ 3.30 (4H, bs, C*H*$_2$–NH, linker), δ 3.58 (8H, bs, C*H*$_2$–N, pyrrolidine), δ 7.20 (2H, bs, N*H*). ^{13}C NMR (100.6 MHz, d^6-DMSO): δ 14.6 (*C*H$_3$–C=N), δ 14.8 (*C*H$_3$–C=N), 25.4 (*C*H$_2$, linker), δ 27.3 (*C*H$_2$, linker), δ 29.9 (*C*H$_2$, pyrrolidine), δ 43.0 (*C*H$_2$–NH, linker), δ 49.4 (*C*H$_2$–N, pyrrolidine), δ 144.9 (*C*=N), δ 175.6 (*C*S). HRMS (+ESI) found mass: 783.1155. Calc. mass for $C_{26}H_{43}N_{12}S_4Zn_2$ (100%, $[M+H^+]^+$): 783.1147. *Anal.* Calc. for $C_{26}H_{42}N_{12}S_4Zn_2{\cdot}2.5H_2O$ (%): C, 37.77; H, 4.84; N, 20.33; S, 15.51. Found: C, 38.39; H, 5.35; N, 19.65; S, 15.67%. IR Data/cm^{-1}: 2928 (m), 2859 (m), 2359 (m), 1435 (vs C=N), 1216 (vs thioamide), 1083 (s), 835 (s, CS). UV–Vis (DMSO): $\lambda_{max}(\varepsilon)$ = 315, 443 nm (13 800, 13 600 M^{-1} cm^{-1}).

2.3. Zinc estimation using ICP-OES

Uptake of zinc complexes was determined by measuring the cellular zinc using ICP-OES. Exponentially growing HepG2 and MCF-7 cells (10 million cells) were incubated with either **6** or **8** (50 μM in zinc) for 1 h at 37 °C. After 1 h, the spent media was removed, washed with PBS (2 × 5 mL) to remove excess complex from extracellular media, scraped and collected in 5 mL PBS. The cells were centrifuged at 2500 rpm for 15 min to get cell pellets, then lysed with 1 M NaOH (0.5 mL) and diluted to 5 mL using 1% (v/v) HNO_3. The solution was subjected to ICP-OES measurement using an instrument that was pre-calibrated for zinc using standard solutions containing 10, 50, 100, 500 and 1000 ppb zinc.

2.4. Ethidium bromide displacement assay

The assay was carried out following previously reported literature procedure [30]. Purity of CT-DNA was evaluated in Milli-Q water from the ratio of absorbance at 260 to 280 nm, which was found to be >1.8, and the concentration was calculated from the absorbance at 260 nm. DNA (424 μM) was added to an aqueous solution containing ethidium bromide and sodium perchlorate (400 mM) until the fluorescence intensity at 602 nm saturated (λ_{ex} = 546 nm). Subsequent addition of zinc complexes **5**–**8** with increasing concentration (0–161.4 μM) quenched the fluorescence. Based on fluorescence quenching, apparent binding constant (K_{app}) was calculated from the equation [EB] × K_{EB} = [complex]$_{50\%}$ × K_{app}, where [EB] denotes the concentration of ethidium bromide and [complex]$_{50\%}$ is the concentration that is required to quench the fluorescence of the DNA-EB adduct by 50% (K_{EB} = 1.0 × 10^7 M^{-1}, [EB] = 2.6 μM).

2.5. DNA viscosity measurement

Viscometric titrations were carried out on a Ubbelohde viscometer at 37 ± 1 °C by varying concentration of zinc complexes **5**–**8** and at fixed concentration of CT-DNA (150 μM) in 5 mM Tris–HCl

(5 mM NaCl) buffer at pH 7.2. Ethidium bromide (EB) and Hoechst 33258 are included for comparison. The flow time was measured after 5 min of incubation with each addition of the zinc complex. Relative viscosities were calculated from the following equation: $\eta = (t-t_0)/t_0$ where, t is the flow time of DNA with or without complex, and t_0 is the flow time of buffer. Finally, relative specific viscosity, $(\eta/\eta_0)^{1/3}$ was plotted versus [compound]/[DNA], where η denotes relative viscosity of the DNA after the addition of complex and η_0 refers to the relative viscosity of DNA alone.

2.6. Circular dichroism study

CD spectra were recorded on a JASCO–J715 spectropolarimeter at room temperature by keeping the concentration of CT-DNA constant (100 μM) and varying the complex concentration from 0 to 100 μM (r_i = ([complex]/[DNA] = 0.0, 0.1, 0.5, 1.0) in 5 mM Tris–HCl buffer (5 mM NaCl, pH 7.2) containing 1% DMSO.

2.7. MTT assay

MTT assay was carried out as described earlier to measure cell viability [30]. Approximately 3000 cells in 100 μL of growth media were seeded in the wells of a 96-well plate. After 24 h, 100 μL of various concentrations of copper bis(thiosemicarbazone) complexes were added and incubated for 48 h at 37 °C in a CO_2 incubator. At the 48th h of incubation, MTT (20 μL of 5 mg/mL) was added to the plate. The contents of the plate were pipetted out carefully and the formazan crystals formed were dissolved in 200 μl of DMSO, the absorbance was measured at 550 nm in a microplate reader (Molecular Devices, Spectramax M5^e). A graph of the concentration versus percentage cell viability was plotted and the concentration at which 50% cell death occurred was used as the IC_{50} value.

2.8. DNA cleavage experiments

The DNA cleavage activity of the bis(thiosemicarbazone) ligands and their zinc complexes were studied using supercoiled pBR322 DNA by agarose gel electrophoresis. Stock solutions of DNA, prepared in Milli-Q water (final DNA concentration of ~36 μM; 4 μL), were incubated with ligand/zinc complex (200 μM; 4 μL) for 4 h in 20 mM HEPES buffer, pH 7.2 at 37 °C. Complex $[Cu(phen)_2](NO_3)_2$ was used as a positive control. After incubation for the indicated time, loading buffer (4 μL) containing 10 mM Tris–HCl, 0.1 M EDTA, 0.25% bromophenol blue was added and frozen at −20 °C for 30 min to quench the reaction. Each reaction mixture (7 μL) was loaded on the agarose gel (1%) and electrophoresized for 3 h under dark condition at 50 V in TAE buffer (40 mM Tris, 20 mM acetic acid, 1 mM EDTA). The gel was stained with ethidium bromide in Milli-Q water (1 μg/mL) for 30 min and destained in Milli-Q water for 4 h and then photographed under UV light. Percentage of cleaved DNA was estimated by measuring relative intensities of supercoiled (SC) and nicked-circular (NC) DNA bands using BioRad Gel Doc XR software.

3. Results and discussion

3.1. Synthesis and characterization

Bis(thiosemicarbazone) ligands **1**–**4** were synthesized, in fairly good yields, by using literature procedures after minor modifications as shown in Scheme 1 [35]. Synthetic routes of the precursor thiosemicarbazides are depicted in Supplementary material as Schemes S1 and S2. Dinuclear zinc complexes **5**–**8** were readily prepared from the corresponding ligands **1**–**4** by refluxing with zinc acetate in ethanol. All bis(thiosemicarbazone) ligands and their dinuclear zinc complexes were characterized by routine spectroscopic techniques, and their purity was assessed by CHN analysis (Fig. 2).

To determine the coordination mode of the ligand with zinc, infrared spectra were recorded for all the ligands and their zinc complexes. Upon complexation with zinc the characteristic stretching frequencies of C=N (1540–1523 cm^{-1}) and C=S (896–835 cm^{-1}) in the ligands were shifted to lower wave numbers in the complexes (1491–1486 cm^{-1} for C=N and 830–797 cm^{-1} for

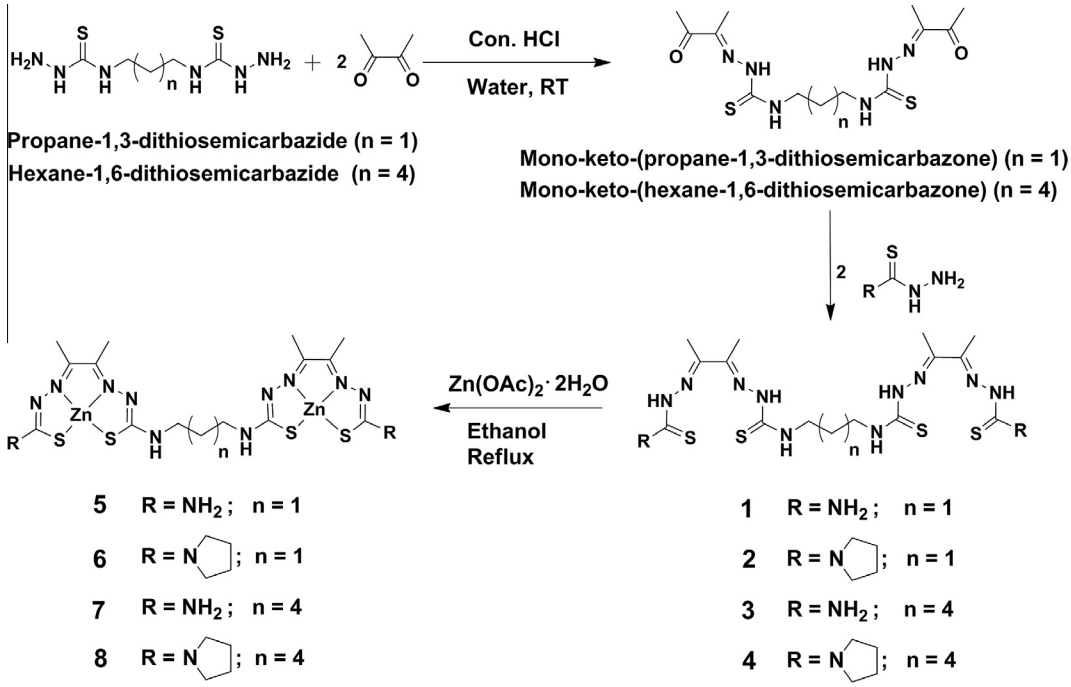

Scheme 1. Synthetic strategy used in the preparation of dinucleating bis(thiosemicarbazone) ligands and their zinc complexes.

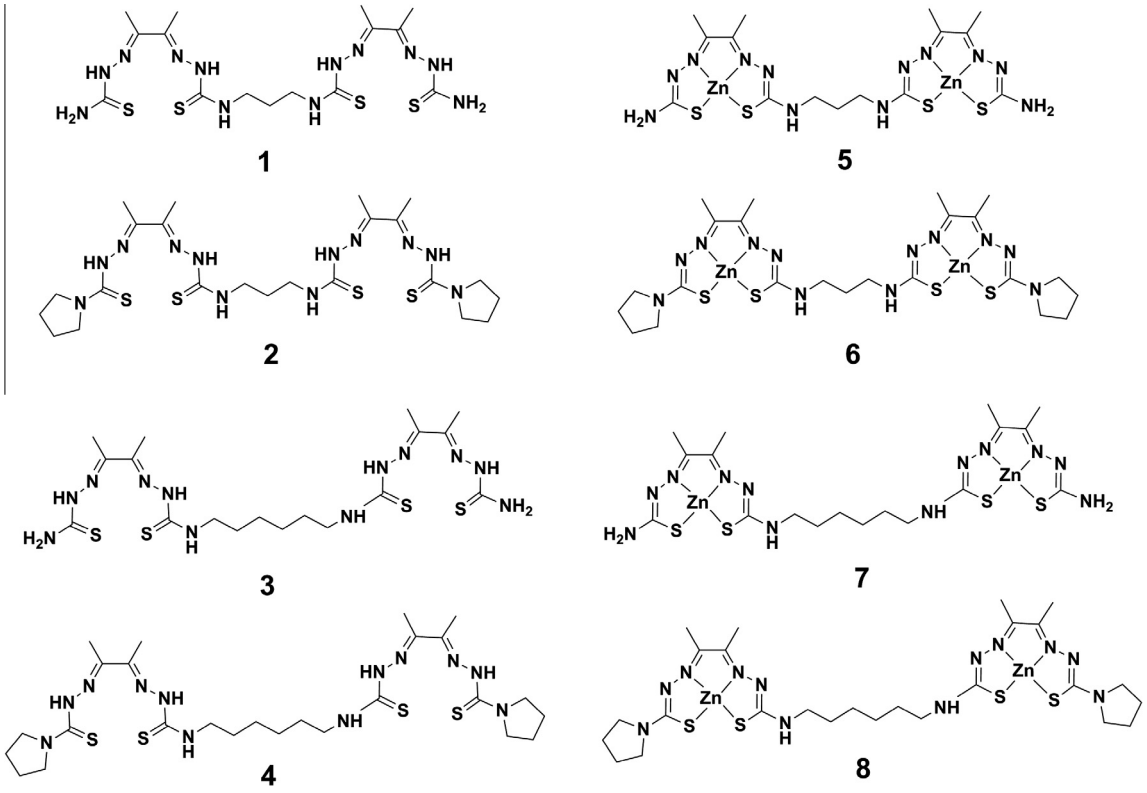

Fig. 2. Proposed molecular structures of bis(thiosemicarbazone) ligands **1**–**4** and their dinuclear zinc complexes **5**–**8**.

C═S), indicating N_2S_2 mode of coordination. It is evident from ^{1}H NMR spectra that all ligands form neutral complexes with zinc by losing four C(S)NH═C hydrogens that resonate between 10 and 11 ppm. The neutral nature of zinc complexes was verified by measuring the molar conductance in DMSO (1 mM in zinc) at room temperature. Complexes **5**, **6**, **7** and **8** showed low molar conductances of 12, 10, 10 and 11 S m^2 M^{-1}, respectively, whereas $[Cu(phen)_2](NO_3)_2$, a known 1:2 electrolyte, showed a molar conductance of 72 S m^2 M^{-1} under similar conditions, confirming the neutral nature of zinc complexes. High-resolution electrospray ionization mass spectra (HR-ESI-MS) showed monoprotonated ($[M+H^+]^+$) or monosodiated ($[M+Na^+]^+$) peaks as the major species in all the solutions of ligands and zinc complexes. Their isotopic distributions conformed to the theoretically calculated isotopic patterns.

It is interesting to note from ^{1}H NMR spectra of the ligands **1** and **3** that NH_2 protons displayed two singlets in the range of δ 7.84–7.86 and δ 8.40–8.41 ppm in 1:1 ratio, evidencing existence of partial double bond character between C and N in S═C–NH_2 that restricts the free rotation around C–N [38]. However, such a double bond character was absent in the zinc complexes **5** and **7** as the NH_2 protons exhibited single peak at δ 6.89 ppm.

3.2. UV–Vis and fluorescence studies

The absorption spectra of ligands and their dinuclear zinc complexes were recorded in DMSO (20 μM), and the representative spectra are shown in Fig. 3A. All ligands displayed an intense band centered at 337 nm along with a shoulder at 346 nm, assigned to $n \rightarrow \pi^*$ transitions of azomethine and thioamide, which is blue shifted by ca. 30 nm with hypochromism upon complexation with

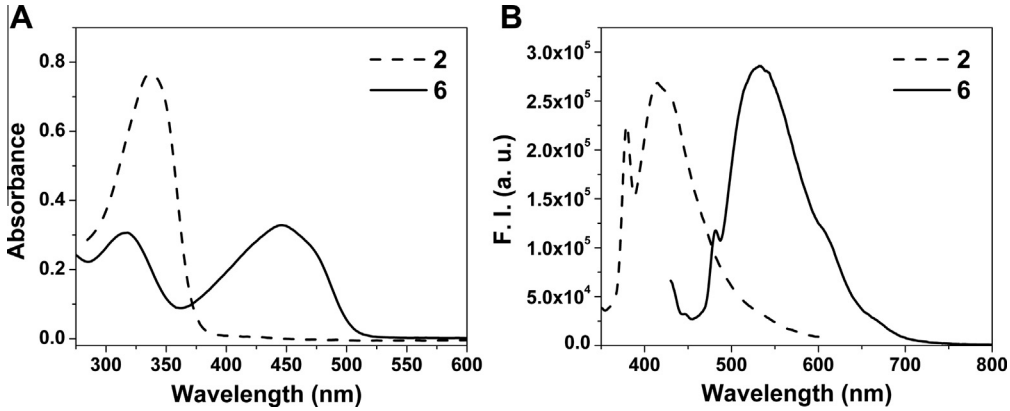

Fig. 3. UV–Vis spectra (A) and fluorescence spectra (B) of the ligand **2** (λ_{ex} = 340 nm) and its zinc complex **6** (λ_{ex} = 420 nm) in DMSO (20 μM in bis(thiosemicarbazone) or in zinc).

Table 1
Photophysical properties of dinuclear zinc complexes.

Complexes	Absorbance λ_{max} (nm) ($\varepsilon \times 10^4$ M^{-1} cm^{-1})	Emission[a] λ_{max} (nm)	Quantum yield[b] $\Phi \times 10^{-3}$	Optical brightness ($\varepsilon \times \Phi$, M^{-1} cm^{-1})
5	312 (1.71), 435 (1.67)	525	1.5	22.4
6	316 (1.53), 445 (1.65)	530	2.4	31.9
7	310 (1.45), 435 (1.33)	525	1.6	19.4
8	315 (1.30), 443 (1.50)	530	2.4	27.2

[a] Emission spectra were measured in DMSO solvent with 420 nm excitation at 5 nm slit width.
[b] Quantum yield was calculated using $[Ru(bpy)_3](PF_6)_2$ ($\Phi = 42 \times 10^{-3}$) as a standard.

zinc, indicating the coordination of azomethine nitrogen and CS sulfur to zinc [39]. We observed an additional low energy absorption band at ca. 440 nm in zinc complexes. The new band is ascribed to sulfur to zinc charge transfer (LMCT) transition.

Several zinc bis(thiosemicarbazone) complexes are known to exhibit weak fluorescence [25,28,30], therefore we measured the fluorescence spectra of ligands **1**–**4** and the corresponding zinc complexes **5**–**8** in DMSO following excitation at 340 and 420 nm, respectively, and the representative spectra are shown in Fig. 3B. The photophysical properties of **5**–**8** are listed in Table 1. Invariably, all the ligands exhibited an emission at 415 nm, while the zinc complexes exhibited emission at longer wavelengths, with a red shift of 115–120 nm. Complexes **6** and **8** exhibited an emission centered at 530 nm which is 5 nm greater than what is observed for **5** and **7**. The quantum yields for zinc complexes were determined using $[Ru(bpy)_3](PF_6)_2$, as a standard for which a quantum yield (Φ) of 42×10^{-3} has been reported [40,41]. Complexes **6** and **8** having a pyrrolidine substituent on the thiosemicarbazide fragment exhibited a quantum yield of 2.4×10^{-3} which is about 1.5 times higher than that of analogous complexes **5** and **7**, and comparable to that of $[(Zn(GTSC)]_3$, whose quantum yield was reported to be 3.0×10^{-3} and displayed intracellular fluorescence [30]. Hence these complexes are anticipated to show fluorescence in cells.

3.3. Cytotoxicity studies

Cytotoxicity was screened initially for all compounds against a range of human cancer cell lines, derived from five different tissue types that include SiHa (cervical cancer), MCF-7 (breast cancer), PC-3 (prostate cancer), A-2780 (ovarian cancer) and HepG2 (hepatocellular liver cancer) using a colorimetric based sulphorhodamine-B (SRB) assay. These cell lines were treated with compounds at 10^{-4}, 10^{-5}, 10^{-6} and 10^{-7} M and the growth inhibition (GI_{50}) was measured at 48 h after staining with SRB. Adriamycin, an anthracycline based anticancer drug, was used as a positive control. The GI_{50} values, corresponding to the cytotoxic activity, are presented in Table 2. The cytotoxicity in HepG2 cells revealed that the ligand **2** and its zinc complex **6** are quite cytotoxic, with a GI_{50} value of <0.1 μM. Their potency is greater than all other analogous compounds tested, and is similar to that of adriamycin. When the measurement was extended to four other cell lines, only **6** exhibited significant cytotoxicity (<0.1 μM) against the MCF-7 cell line, and is comparable to the cytotoxicity caused by adriamycin. We also measured the cytotoxicity of all compounds by MTT assay against MCF-7 and HepG2 cell lines. The cytotoxicity values obtained are represented as IC_{50} and are tabulated in Table S1 (Supplementary material). Complex **6** was found to be the most cytotoxic complex, with IC_{50} values of 12.34 ± 4.92 μM against HepG2 cells and 11.00 ± 4.20 μM against MCF-7 cells. Based on the cytotoxicity we selected **6** for further studies to probe its interaction with DNA and its cellular uptake.

Table 2
The GI_{50} of dinucleating bis(thiosemicarbazone) ligands and their zinc complexes as measured by SRB assay.

Compounds	GI_{50}[a] (μM)				
	SiHa	MCF-7	PC-3	A-2780	HepG2
1	n.d.	n.d.	n.d.	n.d.	>100
2	>100	36.6	70.4	61.0	<0.1
3	>100	>100	>100	>100	>100
4	>100	>100	>100	>100	>100
5	n.d.	n.d.	n.d.	n.d.	>100
6	41.8	<0.1	50.6	34.2	<0.1
7	>100	47.0	>100	75.0	>100
8	>100	>100	>100	>100	>100
Adriamycin[b]	<0.1	<0.1	<0.1	<0.1	<0.1

n.d. = Not determined.
Data are presented as a mean of three independent experiments.
[a] Refers to the amount of drug (μM in bis(thiosemicarbazone) or in zinc) required to inhibit 50% cell growth in 48 h.
[b] Adriamycin was included for comparison.

3.4. Cellular uptake of zinc in cells

To verify the importance of cellular uptake, and its correlation with cytotoxic activity, exponentially growing MCF-7 and HepG2 cells were treated with zinc complexes **6** and **8** (50 μM in zinc) for 60 min at 37 °C and the accumulation of zinc concentration in the cell was estimated using inductively coupled plasma-optical emission spectrometry (ICP-OES). In this study, DMSO (0.5% in OptiMEM media) treated cells were used as a vehicle control. To obtain the detectable amount of zinc by the ICP-OES technique, cells were incubated with complexes for a short time (1 h), but at much higher concentration (50 μM in zinc) than the observed IC_{50}. The treatment of complexes **6** and **8** significantly increases the zinc concentration in cells compared to untreated cells (Fig. 4) that suggests the facile intake of complexes. Interestingly both cytotoxic complex **6** and non-cytotoxic complex **8** accumulate the same amount of zinc within MCF-7 and HepG2 cell lines in spite of their different cytotoxicity. This result suggests that differences in cellular uptake are not causing differences in their cytotoxicity. The intracellular behavior is likely to be significantly different for these two complexes.

3.5. Cellular fluorescence studies by flow cytometry

As the most cytotoxic complex was also the most fluorescent complex **6**, we investigated the ability of the complex to fluoresce within the cell. We treated HepG2 cells for a short time, 30 min, at room temperature with 20 μM and 50 μM of complex **6** in PBS buffer, pH 7.2 containing 1% DMSO. Cells that were treated with DMSO (1% DMSO in PBS buffer) were used as a control. Fluorescence from the cell was measured using a flow cytometer following excitation at 488 nm. As shown in Fig. 5, the complex **6** treated cells exhibited only 1.4–1.5-fold fluorescence enhancement compared to autofluorescence (DMSO treated cells) at both 20 and 50 μM. These results suggest that **6** does not exhibit fluorescence in the cell though the fluorescence quantum yield in DMSO is comparable with $[Zn(GTSC)]_3$, a bis(thiosemicarbazone) complex that displayed

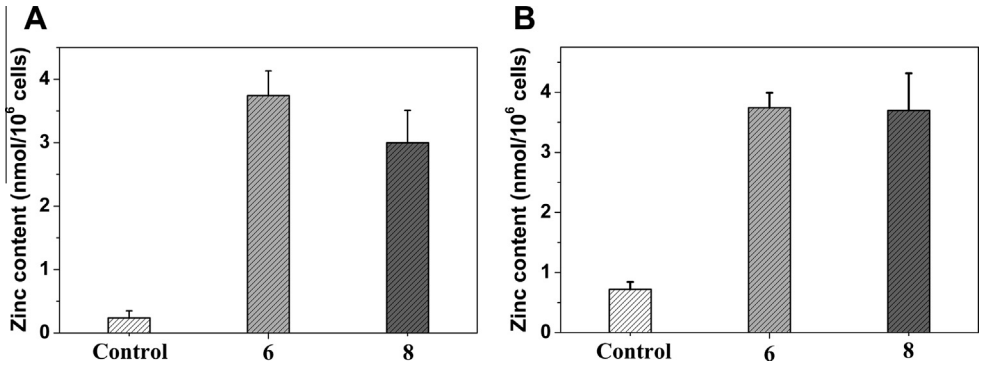

Fig. 4. Cellular zinc content was estimated in MCF-7 cells (panel A) and HepG2 cells (panel B) using inductively coupled plasma optical emission spectrometry after treatment of DMSO (0.5% in OptiMEM media) as a control, **6** and **8** (50 μM in zinc) for 1 h at 37 °C. Error bars indicate ± standard deviations for three experiments.

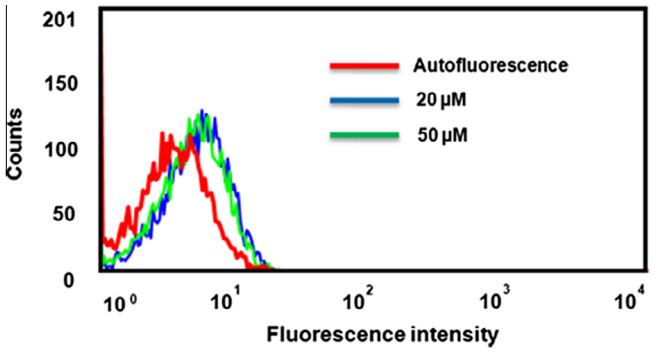

Fig. 5. HepG2 cells were incubated either with **6** at 20 and 50 μM (in zinc) or with DMSO (1% in PBS) for 30 min at room temperature and fluorescence was recorded using a flow cytometer following excitation at 488 nm.

Table 3
Binding constants of **5**–**8** (in zinc) with CT-DNA.[a]

Complexes	K_{app} ($\times 10^4$ M^{-1})
5	6.4 ± 0.1
6	7.4 ± 0.2
7	9.2 ± 0.1
8	12.8 ± 0.2

[a] Each value is the average value from two sets of experiments.

good fluorescence in several cancer cell lines [30]. The poor fluorescence response in the cell is possibly due to the quenching of fluorescence in aqueous environments. To validate this hypothesis, fluorescence spectra was recorded for **6** at 20 μM and 50 μM in the cuvette at various compositions of DMSO and PBS buffer (0–99%) following excitation at 420 and 488 nm (Fig. S1, Supplementary material). We observed significant quenching (84–94%) in the fluorescence intensity of **6** (λ_{ex} = 488 nm) when the percentage of PBS buffer increased to 98% in DMSO. This suggests that fluorescence quenching is associated with aqueous quenching, which would result in poor fluorescence inside the cell.

3.6. DNA interaction studies

3.6.1. DNA binding

DNA is one of the major targets for several anticancer active compounds including metal complexes [42–45]. The increased activity of dinuclear or multinuclear platinum complexes compared to cisplatin could be traced to the ability of the molecule to bind DNA in a specific fashion [46]. Therefore, we investigated the ability of metal complexes **5**–**8** to interact with calf-thymus DNA by ethidium bromide displacement assay using fluorescence spectroscopy. Incremental addition of complexes to a solution containing EB-DNA mixture (fluorescent adduct) quenches the fluorescence gradually by displacing EB from DNA. The apparent binding constants (K_{app}) were estimated from the concentration needed to 50% fluorescence quenching. K_{app} values are presented in Table 3 and a representative diagram is depicted in Fig. 6. All complexes exhibited good binding efficacy to DNA, with K_{app} varying in the narrow range of 6.4×10^4 M^{-1} to 12.8×10^4 M^{-1}. These binding constants are in the same range of mononuclear zinc complexes [30]. It was noticed that the pyrrolidinylthiosemicarbazide based complexes possess marginally superior binding propensities over the thiosemicarbazide based complexes. Overall, the DNA interaction studies suggest that the zinc complexes interact with DNA *via* electrostatic interaction similar to that of mononuclear zinc diacetylbis(4-methyl-3-thiosemicarbazone) [Zn(ATSM)] [25].

3.6.2. Viscosity measurements

To understand the nature of interaction between zinc complexes **5**–**8** and DNA, viscosity experiments were carried out on a Ubbelohde viscometer at 37 °C by varying concentration of zinc complexes versus CT-DNA. Hydrodynamic experiments such as viscosity and sedimentation methods are sensitive to DNA length. Classical mode of interactions like intercalation increases the viscosity by increasing the distance between base pairs, which in turn increases the overall length of DNA. Conversely, non classical mode of interactions such as electrostatic and groove binding causes the reduction or no change in the DNA viscosity with different concentrations. The effect of zinc complexes or EB or Hoechst 33258 on the relative viscosities of CT-DNA solution is shown in Fig. 7. As expected, the EB, a classical intercalator, dramatically increases the contour length of the DNA and thereby its viscosity. On the other hand, Hoechst 33258, a known minor groove binder, does not elongate DNA and causes a slight decrease in the viscosity (Fig. 7). However, the addition of increasing amounts of zinc complexes to DNA solution does not increase the relative viscosity significantly, indicating that the zinc complexes interact with DNA neither by intercalation nor is it a minor groove binder like Hoechst 33258. This result supports our DNA binding studies that weak electrostatic interactions between the negatively charged DNA and the positively polarized zinc, which has a vacant coordination site in the complex, is preferred over other interactions.

3.6.3. Circular dichroism studies

To examine if binding of zinc complexes to DNA causes changes in the conformation of DNA, circular dichroism (CD) studies were

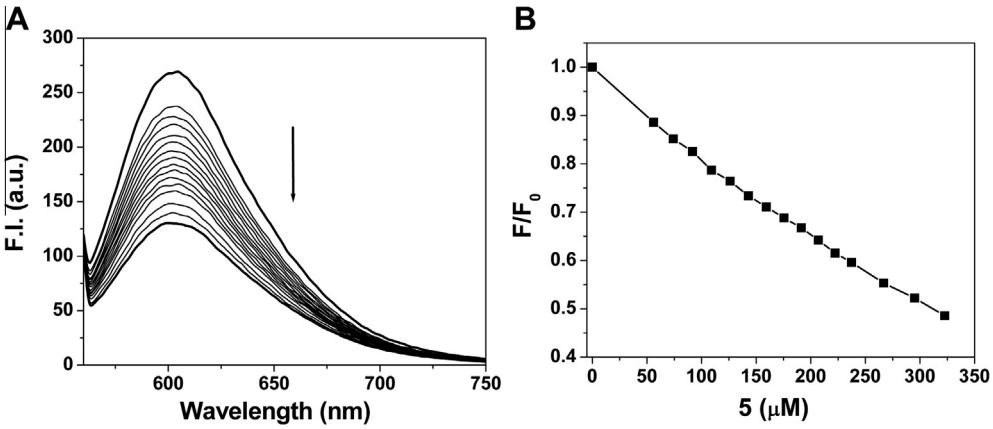

Fig. 6. DNA binding behavior of dinuclear zinc complexes as measured by ethidium bromide displacement assay. (A) Addition of increasing concentrations **5** (0 to 161.4 μM) to DNA-EB mixture (DNA = 424 μM; EB = 2.6 μM) in aqueous $NaClO_4$ (400 mM) solution quenches the fluorescence. (B) A plot of F/F_0 vs. complex concentration at 602 nm (λ_{ex} = 546 nm).

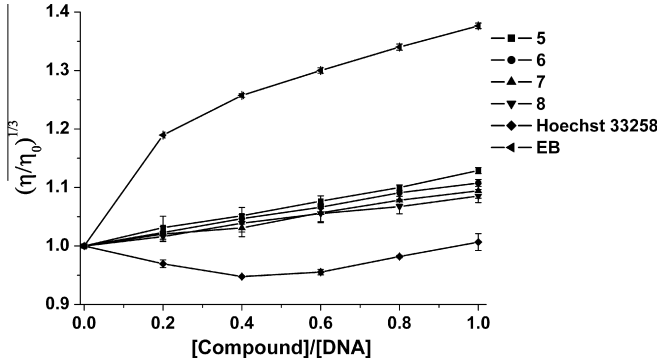

Fig. 7. Effect of complexes **5**–**8** on the relative viscosity of CT-DNA. Complexes **5**–**8** were added at increasing concentrations (0, 30, 60, 90, 120, 150 μM in zinc) to CT-DNA (150 μM) at 37 °C in 5 mM Tris–HCl buffer (5 mM NaCl) at pH 7.2. Data shown is an average of three experiments ± SD.

Table 4
In vitro pBR322 DNA cleavage by bis(thiosemicarbazone) ligands **1**–**4** and their zinc complexes **5**–**8** at 200 μM.

Compounds	% DNA cleavage[a]
1	38
2	39
3	39
4	[b]
5	[b]
6	35
7	33
8	33

[a] DNA alone rendered an average cleavage of 25%.
[b] Percentage of cleavage could not be determined due to precipitation.

carried out with CT-DNA in the absence or in the presence of increasing concentrations of zinc complexes **6** and **8** (Fig. 8). CD spectrum of CT-DNA in Tris–HCl buffer (5 mM) displayed a positive band centered at 275 nm due to base stacking and a negative band centered at 248 nm due to right-handed helicity of DNA [47]. These bands are characteristic for DNA in the right-handed B form. Apparently the addition of zinc complexes to CT-DNA at different [complex]/[CT-DNA] ratios (0.0, 0.1, 0.5 and 1.0) do not show any significant changes in base stacking or in helicity. This type of a behavior is typical of electrostatic interaction between metal complexes and DNA [48]. Moreover this result is consistent with our DNA binding and viscosity studies.

3.6.4. DNA cleavage studies

We also probed the ability of the complexes to cleave DNA by agarose gel electrophoresis after incubating compounds **1**–**8** with supercoiled pBR322 plasmid DNA for 4 h at 37 °C (Fig. S2 and S3,

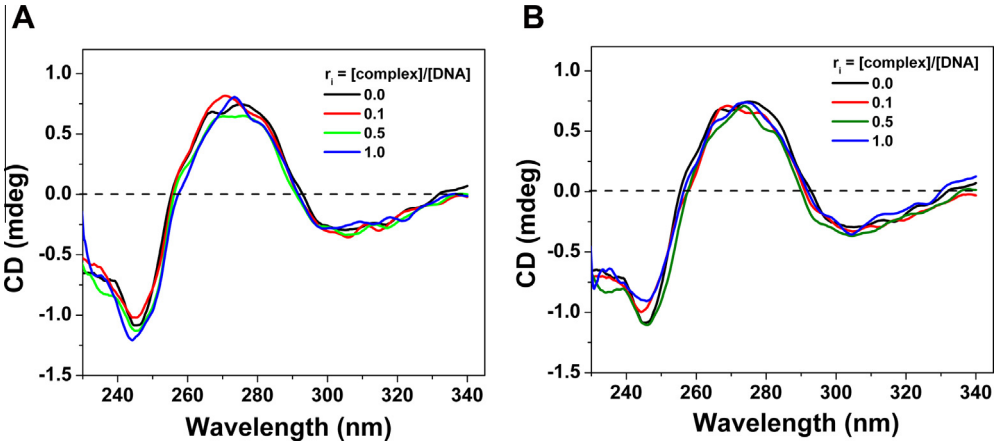

Fig. 8. CD spectra of CT-DNA (100 μM) in 5 mM Tris–HCl buffer (5 mM NaCl, pH 7.2), in the absence and in the presence of increasing concentrations (0, 10, 50 and 100 μM) of **6** (A) and **8** (B) to DNA (r_i = [complex]/[DNA] = 0.0, 0.1, 0.5 and 1.0).

Supplementary material). Apparently, neither the ligand nor the zinc complex cleaves even 50% of DNA at 200 μM (Table 4). In contrast, $[Cu(phen)_2](NO_3)_2$, a positive control, cleaves ~80% DNA at 20 μM. These results suggest that both ligands and their zinc complexes do not manifest their cytotoxicity through DNA cleavage.

4. Conclusion

We have synthesized a family of interesting dinuclear zinc bis(thiosemicarbazone) complexes with varying length of the linker connecting the two bis(thiosemicarbazone) moieties and the nature of the substituents on the thiosemicarbazide part of the ligand. These zinc complexes displayed green fluorescence in DMSO but not in the cell or in aqueous media. Cytotoxicity studies against a range of cancer cell lines reveal that only complex 6 is significantly anticancer active, suggesting that the cytotoxicity is dependent on several factors including the length of the carbon chain linker and substituents on the thiosemicarbazide. In MCF-7 and HepG2 cells, both complexes 6 and 8 are taken up in similar amounts. Based on DNA binding assessed by ethidium bromide displacement assay, viscosity analysis, CD spectral analysis and DNA cleavage studies we conclude that these complexes effectively interact with DNA in an electrostatic manner without causing any DNA cleavage. Mechanistic studies are underway to elucidate the root of cytotoxicity at the cellular level.

Acknowledgements

D. P. thanks Council of Scientific and Industrial Research (CSIR), New Delhi for senior research fellowship. Authors acknowledge Department of Science and Technology (DST), New Delhi for research grant. We thank Prof. K. Somasundaram and Ms. V. S. Sridevi, Department of Microbiology and Cell Biology, Indian Institute of Science (IISc) for MTT and flow cytometry data. We thank Prof. S. P. Sharma, Department of Molecular Biophysics Unit (MBU), IISc for help in obtaining CD data.

Appendix A. Supplementary material

Supplementary data associated with this article can be found, in the online version, at http://dx.doi.org/10.1016/j.ica.2013.09.014.

References

[1] B. Rosenberg, L. VanCamp, J.E. Trosko, V.H. Mansour, Nature 222 (5191) (1969) 385.
[2] R.A. Alderden, M.D. Hall, T.W. Hambley, J. Chem. Educ. 83 (2006) 728.
[3] K.J. Kilpin, P.J. Dyson, Chem. Sci. 4 (2013) 1410.
[4] C.G. Hartinger, N. Metzler-Nolte, P.J. Dyson, Organometallics 31 (2012) 5677.
[5] J. Zhang, F. Zhang, H. Li, C. Liu, J. Xia, L. Ma, W. Chu, Z. Zhang, C. Chen, S. Li, S. Wang, Curr. Med. Chem. 19 (2012) 2957.
[6] P.C.A. Bruijnincx, P.J. Sadler, Curr. Opin. Chem. Biol. 12 (2008) 197.
[7] M. Galanski, Curr. Med. Chem. 12 (2005) 2075.
[8] S. van Zutphen, J. Reedijk, Coord. Chem. Rev. 249 (2005) 2845.
[9] N.J. Wheate, S. Walker, G.E. Craig, R. Oun, Dalton Trans. 39 (2010) 8113.
[10] N.P.E. Barry, P.J. Sadler, Chem. Commun. 49 (2013) 5106.
[11] Available from: <http://www.clinicaltrials.gov/>.
[12] Available from: <http://www.cancer.gov/>.
[13] J.D. Roberts, J. Peroutka, N. Farrell, J. Inorg. Biochem. 77 (1999) 51.
[14] M.-G. Mendoza-Ferri, C.G. Hartinger, R.E. Eichinger, N. Stolyarova, K. Severin, M.A. Jakupec, A.A. Nazarov, B.K. Keppler, Organometallics 27 (2008) 2405.
[15] C. Manzotti, G. Pratesi, E. Menta, R. Di Domenico, E. Cavalletti, H.H. Fiebig, L.R. Kelland, N. Farrell, D. Polizzi, R. Supino, G. Pezzoni, F. Zunino, Clin. Cancer Res. 6 (2000) 2626.
[16] K. Suntharalingam, A.J.P. White, R. Vilar, Inorg. Chem. 49 (2010) 8371.
[17] P. Molenveld, J.F.J. Engbersen, H. Kooijman, A.L. Speck, D.N. Reinhoudt, J. Am. Chem. Soc. 120 (1998) 6726.
[18] X.-L. Zhao, Z.-S. Li, Z.-B. Zheng, A.-G. Zhang, K.-Z. Wang, Dalton Trans. 42 (2013) 5764.
[19] A. Medina-Molner, B. Spingler, Chem. Commun. 48 (2012) 1961.
[20] J.R. Dilworth, R. Hueting, Inorg. Chim. Acta 389 (2012) 3.
[21] A.K. Nandi, S. Chaudhuri, S.K. Mazumdar, S. Ghosh, Inorg. Chim. Acta 92 (1984) 235.
[22] D.X. West, A.E. Liberta, S.B. Padhye, R.C. Chikkate, P.B. Sonawane, A.S. Kumbhar, R.G. Yerande, Coord. Chem. Rev. 123 (1993) 49.
[23] E. Lopez-Torres, M.A. Mendiola, Inorg. Chim. Acta 363 (2010) 1735.
[24] B.M. Paterson, P.S. Donnelly, Chem. Soc. Rev. 40 (2011) 3005.
[25] A.R. Cowley, J. Davis, J.R. Dilworth, P.S. Donnelly, R. Dobson, A. Nightingale, J.M. Peach, B. Shore, D. Kerr, L. Seymour, Chem. Commun. (2005) 845.
[26] I.H. Hall, C.B. Lackey, T.Y. Kistler, J.S. Ives, H. Beraldo, L.J. Ackerman, D.X. West, Arch. Pharm. Pharm. Med. Chem. 333 (2000) 217.
[27] C.R. Kowol, R. Trondl, V.B. Arion, M.A. Jakupec, I. Lichtscheidl, B.K. Keppler, Dalton Trans. 39 (2010) 704.
[28] S.I. Pascu, P.A. Waghorn, T.D. Conry, B. Lin, H.M. Betts, J.R. Dilworth, R.B. Sim, G.C. Churchill, F.I. Aigbirhio, J.E. Warren, Dalton Trans. 16 (2008) 2107.
[29] D. Palanimuthu, S.V. Shinde, D. Dayal, K. Somasundaram, A.G. Samuelson, Eur. J. Inorg. Chem. (2013) 3542.
[30] D. Dayal, D. Palanimuthu, S.V. Shinde, K. Somasundaram, A.G. Samuelson, J. Biol. Inorg. Chem. 16 (2011) 621.
[31] D. Palanimuthu, S.V. Shinde, K. Somasundaram, A.G. Samuelson, J. Med. Chem. 56 (2013) 722.
[32] S.I. Pascu, P.A. Waghorn, T.D. Conry, H.M. Betts, J.R. Dilworth, G.C. Churchill, T. Pokrovska, M. Christlieb, F.I. Aigbirhio, J.E. Warren, Dalton Trans. (2007) 4988.
[33] A.I. Matesanz, I. Cuadrado, C. Pastor, P. Souza, Z. Anorg. Allg. Chem. 631 (2005) 780.
[34] M. Christlieb, A.R. Cowley, J.R. Dilworth, P.S. Donnelly, B.M. Paterson, H.S.R. Struthers, J.M. White, Dalton Trans. (2007) 327.
[35] M. Christlieb, H.S.R. Struthers, P.B. Bonnitcha, A.R. Cowley, J.R. Dilworth, Dalton Trans. (2007) 5043.
[36] M.L. Duran, A. Sousa, J. Romero, A. Castineiras, E. Bermejo, D.X. West, Inorg. Chim. Acta 294 (1999) 79.
[37] E.L. Torres, M.A. Mendiola, C.J. Pastor, B.S. Perez, Inorg. Chem. 43 (2004) 5222.
[38] P. Tarasconi, S. Capacchi, G. Pelosi, M. Cornia, R. Albertini, A. Bonati, P.P. Dall'Aglio, P. Lunghi, S. Pinelli, Bioorg. Med. Chem. 8 (2000) 157.
[39] A. Castineiras, E. Bermejo, D.X. West, L.J. Ackerman, Polyhedron 18 (1999) 1463.
[40] J.V. Caspar, T.J. Meyer, J. Am. Chem. Soc. 105 (1983) 5583.
[41] A.T.R. Williams, S.A. Winfield, J.N. Miller, Analyst 108 (1983) 1067.
[42] A.C. Komor, J.K. Barton, Chem. Commun. 49 (2013) 3617.
[43] L.H. Hurley, Nat. Rev. Cancer 2 (2002) 188.
[44] E. Gallori, C. Vettori, E. Alessio, F.G. Vilchez, R. Vilaplana, P. Orioli, A. Casini, L. Messori, Arch. Biochem. Biophys. 376 (2000) 156.
[45] K.E. Erkkila, D.T. Odom, J.K. Barton, Chem. Rev. 99 (1999) 2777.
[46] N.J. Wheate, J.G. Collins, Coord. Chem. Rev. 241 (2003) 133.
[47] C.-Y. Gao, X. Qiao, Z.-Y. Ma, Z.-G. Wang, J. Lu, J.-L. Tian, J.-Y. Xu, S.-P. Yan, Dalton Trans. 41 (2012) 12220.
[48] N. Shahabadi, M. Falsafi, N.H. Moghadam, J. Photochem. Photobiol. B: Biol. 122 (2013) 45.